Sensorless Rotor Position Estimation of an Interior Permanent-Magnet Motor From Initial States

Jung-Ik Ha, *Member, IEEE*, Kozo Ide, *Member, IEEE*, Toshihiro Sawa, *Member, IEEE*, and Seung-Ki Sul, *Fellow, IEEE*

***Abstract*—This paper describes a torque, speed, or position control method at standstill and low speed in the interior permanent-magnet motor (IPMM) drive system without any rotational transducer. While IPMMs have originally magnetic saliency, it varies according to the load conditions and the control performance can be easily degraded. In this paper, the saliency or impedance difference is used as the conventional methods and, nevertheless, in order to amplify the difference containing the information of the rotor angle and to maintain a reasonable performance under any load condition a high-frequency injection scheme is proposed. A speed and position estimation scheme based on the characteristics of the high-frequency impedance is proposed. The scheme extracts the high-frequency impedance components related to the rotor position. An initial angle estimation scheme for starting from an arbitrary rotor position is also proposed. It can distinguish the north magnetic pole position from the south one in several decade milliseconds. The proposed scheme enables position control of a transducerless or position-sensorless IPMM. The experimental results clarify the satisfactory operation of the proposed position control algorithm under any load condition.**

***Index Terms*—Motor drives, position estimation, sensorless control.**

I. Introduction

UP TO NOW, the sensorless drive of an interior permanent-magnet motor (IPMM) has been studied in view of the robustness, reliability, cost, and so on. After the 1980s, with developments in power electronics and microelectronics, the sensorless control methods to achieve comparable performance in sensored vector control have been investigated. There are largely two categories in the sensorless position estimation schemes for IPMMs. One is based on back electromotive force (EMF). It uses voltage models [1], [2], observers in the synchronous or stationary frame [3], [4], or Kalman filters [5]. It presents good results in the middle and high-speed regions. Since the amplitude of back EMF is proportional to the rotor speed, it fails in the low-speed region. The others are utilizing the magnetic saliency [6]–[12]. Some algorithms inject voltage signals in a sampling period to estimate rotor position [7], [8]. Since they detect inductance using voltage signals in a short time, they can be frail to parameter variation or measurement noises. The other injects rotating high frequency and uses tracking algorithm [9]. Since it utilizes the rotating high-frequency signal, the dynamic characteristics are restricted within a narrow limit. Recently, a new algorithm based on harmonic signal injection to the motor was proposed for zero- or low-frequency operation [10]–[12]. This method is applied to induction motors and synchronous reluctance motors. It gives reasonable torque control capability at zero and low stator frequency, even under heavily loaded condition. Compared with another signal injection method, it injects not the rotating signal but the fluctuating signal on the flux axis and, hence, it generates less torque ripple, vibration, and audible noise.

This method, using magnetic saliency, still has one problem. This is in the estimation of magnetic pole position at the initial state. The source of the problem is that there are two stable points, the north and south magnetic pole positions. If the estimated angle is aligned at the south magnetic pole position, the sign of output torque will be changed and the system will be unstable. Hence, it is important to distinguish the north magnetic pole position. Ideally, it is impossible to distinguish it between two stable points because the speed of rotor is nearly zero at the initial state and at this time, there is no back-EMF information. Therefore, in order to distinguish the north magnetic pole position, nonideal phenomenon should be considered. The conventional method for the differentiation of the $d$axis, which is identical to the north magnetic pole position, is based on the flux saturation by the rotor flux [13], [14]. Due to the flux saturation, the terminal impedance at the north magnetic pole position decreases but the terminal impedance at the south magnetic pole position increases. Therefore, if the same voltage is injected at the north and south magnetic pole position, the offset current toward the direction, which indicates the north magnetic pole position, will be generated. Since this method uses a low-pass filter to measure the offset current, the response for detection is poor. The other methods for identification of the d axis are based on the phase between voltage and current [15], [16]. The phase is basically determined by the speed of rotor. If the speed of rotor is zero, it has no information about rotor position. The speed ripple by test signals mainly affects these methods. However, there will be no ripple in speed according to the mechanical system or load conditions. In this case, these methods are not effective.

Paper IPCSD 03–013, presented at the 2001 Industry Applications Society Annual Meeting, Chicago, IL, September 30–October 5, and approved for publication in the IEEE TRANSACTIONS ON INDUSTRY APPLICATIONS by the Industrial Drives Committee of the IEEE Industry Applications Society. Manuscript submitted for review October 15, 2001 and released for publication March 5, 2003.

J.-I. Ha is with the Mechatronics Center, Samsung Electronics Company, Gyeonggi 442-742, Korea (e-mail: haji@ieee.org).

K. Ide is with the Mechatronics R&D Department, Yaskawa Electric Company, Kitakyusyu 803-8530, Japan (e-mail: kozo@yaskawa.co.jp).

T. Sawa is with the Tokyo Plant, Yaskawa Electric Company, Saitama 358-8555, Japan (e-mail: sawa@yaskawa.co.jp).

S.-K. Sul is with the School of Electrical Engineering and Computer Science, Seoul National University, Seoul 151-742, Korea (e-mail: sulsk@plaza.snu.ac.kr).

Digital Object Identifier 10.1109/TIA.2003.811781

This paper presents a sensorless control algorithm using high-frequency injection. Since it uses the high-frequency impedance of an IPMM, the characteristics in the high-frequency region are tested and analyzed under various load conditions. To amplify the signals of the characteristics, the injection of fluctuating signals on the d axis in the rotor reference frame is used [8], [9]. IPMMs that have the highest impedance on the q axis can be easily saturated on this axis according to the load level. Therefore, the magnetic saliency will be decreased or will vanish. To avoid the failure of sensorless control for this reason, the compensation using the d-axis current is proposed. Since the adjustment of the d-axis current may make the torque per current of the IPMM to be low, the compensation considering the characteristic is proposed. In the proposed method, the hysteresis phenomenon is used to estimate the north magnetic pole position at the initial state. This method distinguishes the north magnetic pole position. This has fast dynamics and can estimate the accurate magnetic pole position. The proposed estimation of rotor position enables sensorless torque, speed, and position controls under any load conditions. Experimental results clarify the fast and accurate operation of the proposed sensorless algorithm.

II. Characteristics of Torque and High-Frequency Impedance

Fig. 1 shows the test results of an IPM motor whose parameters are listed in Table I. Fig. 1(a) and (b) represents the torque per amplitude of current according to the d- and q-axes currents and the d-axis current generating the maximum torque per current in accordance with q-axis current, respectively. The IPMM makes the magnetic and reluctance torque simultaneously and the high torque per current can be generated such as

$$T_e = \frac{3}{4}P\left\{(L_d - L_q)i_d + K_e\right\}i_q. \tag{1}$$

To obtain the high reluctance torque and to hold high efficiency, the d-axis current can be used as shown in Fig. 1(b).

The equations of the stator terminal voltage are as follows:

$$v_d = Ri_d + L_d p i_d - \omega_r L_q i_q \tag{2}$$

$$v_q = Ri_q + L_q p i_q + \omega_r (L_d i_d + K_e). \tag{3}$$

At zero or low speed the speed voltage terms can be neglected. In this case, if the high-frequency signal is injected, the high-frequency impedance can be expressed as follows:

$$Z_{dh} \approx \frac{v_{dh}}{i_{dh}} = R + L_{dh}\omega_h \tag{4}$$

$$Z_{qh} \approx \frac{v_{qh}}{i_{qh}} = R + L_{qh}\omega_h \tag{5}$$

where L_{dh} and L_{qh} represent d and q-axes inductances at the injected high frequency.

Since the air gap at the d axis is larger than that at q axis from rotor structure, the inductance at the d axis is smaller than that at any other axis. At zero or low speed, the high-frequency impedance is dominated by the inductance. Therefore, the high-frequency impedance measured in the stationary reference frame can be expressed as (6). It can be easily derived from (4) and (5)

$$Z_h(\theta_r) = Z_{ha} - \frac{1}{2}Z_{hp}\cos 2(\theta_r + \phi) \tag{6}$$

where Z_{ha} is the average value of high-frequency impedance, Z_{hp} represents the difference in high-frequency impedances, and ϕ is the angle where minimum high-frequency impedance occurs.

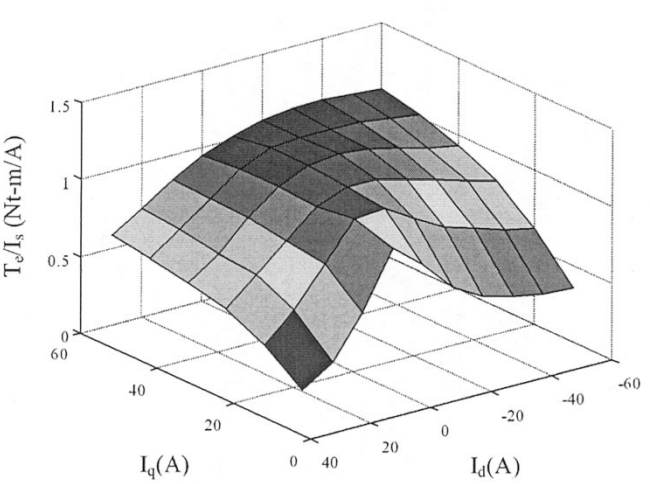

(a)

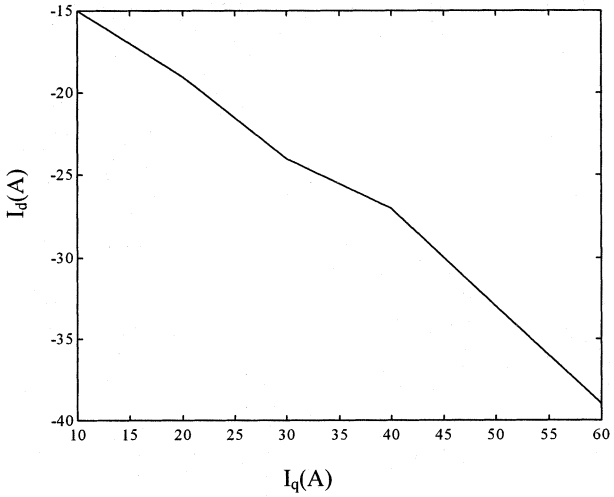

(b)

Fig. 1. Characteristics of output torque. (a) Torque per current according to d- and q-axes currents. (b) d- and q-axes currents at maximum torque per current.

TABLE I
Parameters of an IPM Under Test

Rated Power	11 [kW]
Rated Speed	1750 [rpm]
Number of Poles	6
Rated Line-to-line Voltage	190 [Vrms]
Rated Current	39.5 [Arms]
Stator Resistance, R_s	0.109 [Ω]
D-axis Inductance, L_d	3.60 [mH]
Q-axis Inductance, L_q	4.30 [mH]

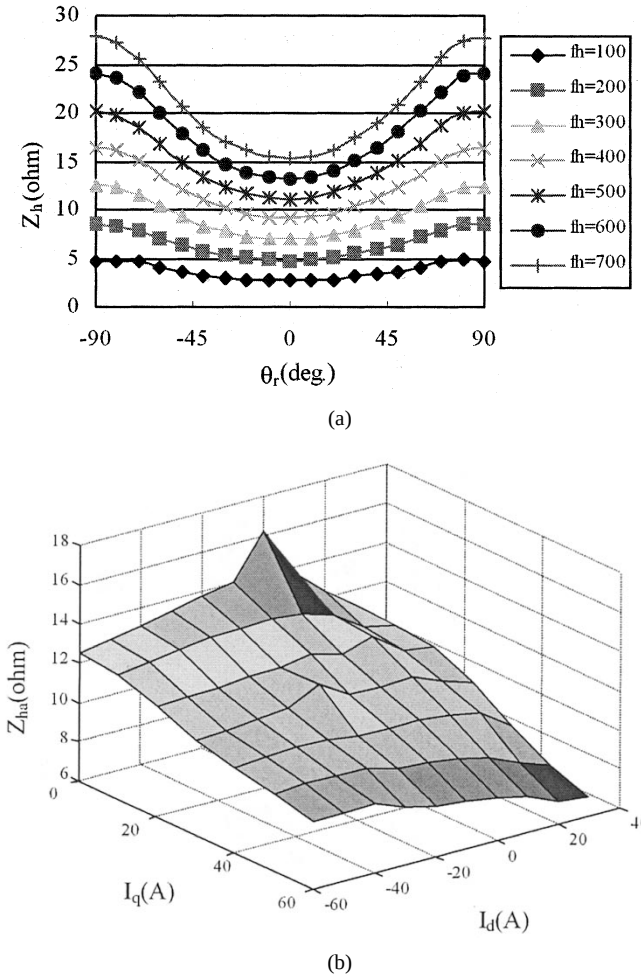

Fig. 2. Impedance of motor under test. (a) Spatial impedance at various frequencies under no-load condition. (b) Average values of high-frequency impedance according to d- and q-axes currents (injection signal: 500 Hz, 30 V).

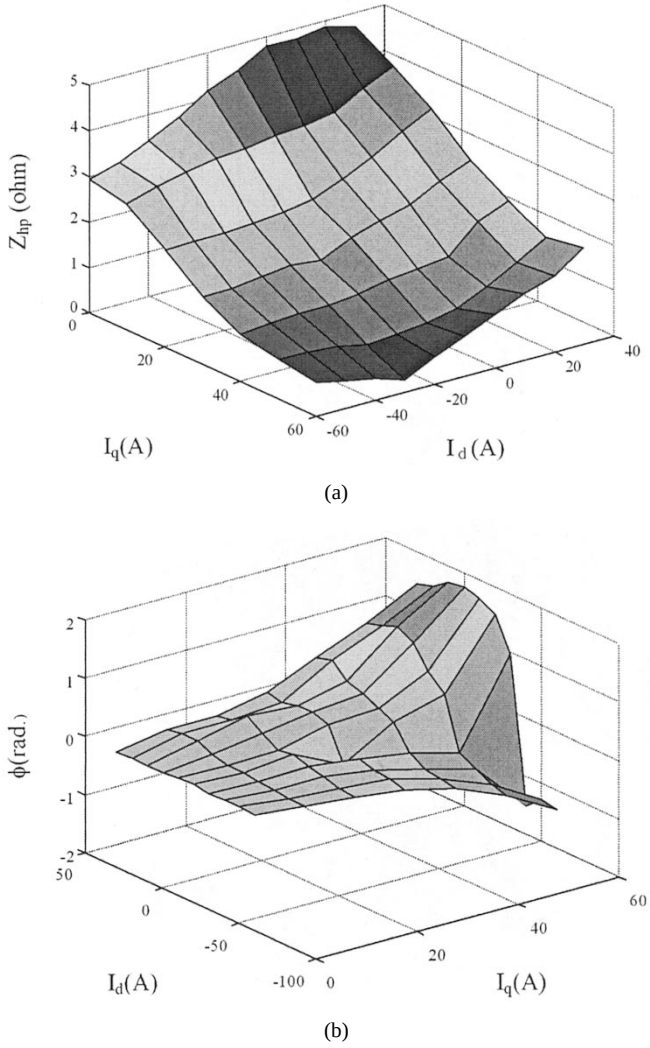

Fig. 3. Characteristics of high-frequency impedance (injection signal: 500 Hz, 30 V). (a) Difference of high-frequency impedances according to d- and q-axes currents. (b) Angle representing minimum value of high-frequency impedance according to d- and q-axes currents.

Fig. 2(a) shows the stator terminal impedance according to the rotor position under no-load condition. To measure the impedance the continuously fluctuating signals in the rotor reference frame are used. As the frequency increases, the impedance difference also increases. The average value Z_{ha} of high-frequency impedance becomes small according to the amplitude of the stator current, as shown in Fig. 2(b). The impedance difference Z_{hp}, representing the degree of magnetic saliency, is also decreasing in accordance with the increase of load current, that is the q-axis current as shown in Fig. 3(a). However, the difference increases as the d-axis current does. It can be explained by considering the spatial magnetic saturation. The angle representing the minimum high-frequency impedance, ϕ, is shifted according to the stator current. It means the angle where the lowest inductance occurs as shown in Fig. 3(b). It results from the saturation by the permanent magnet and stator currents.

III. Control Strategy Using High-Frequency Injection

The sensorless control scheme using high-frequency signal fluctuating in the synchronous reference frame has been proposed [8], [9]. There are voltage and current types in the high-frequency injection methods. The current injection method may have the faster dynamic than the voltage one, but, in the case where the impedance difference decreases according to load condition, the controllability of a current-type injection system can be easily lost under heavy-load condition. The voltage injection method is appropriate in this motor. Fig. 4 shows the block diagram of the proposed sensorless algorithm. In utilizing the signals of impedance difference as shown Fig. 2(a), the rotating injection signal makes larger torque ripples [9]. The fluctuating signal on the q axis makes a constant torque ripple but its level is very high [10]. For this reason, the high-frequency signal fluctuating in the rotor reference frame is adopted to reduce torque ripples by an injected signal. The field-orientation control (FOC) consists of the preprocessor extracting the high-frequency impedance component and the correction controller estimating the rotor angle and speed. If the voltage signal of $v_{dh}^* = V_{dh}^* \sin(\omega_h t)$ is injected, the preprocessor extracts the square of

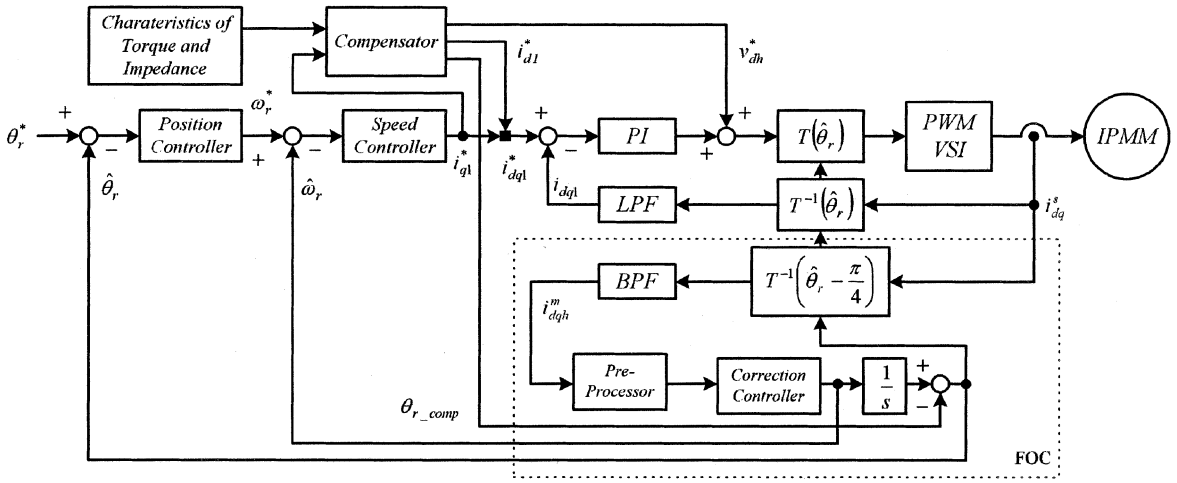

Fig. 4. Block diagram of sensorless control scheme using high-frequency voltage signal injection.

amplitude of injected current components and the input of correction controller is as follows:

$$\begin{aligned}\mathrm{Err} &\equiv \left|i_q^m\right|^2 - \left|i_d^m\right|^2 \\ &\approx \frac{{V_{dh}^*}^2 Z_{ha} Z_{hp} \sin 2(\theta_r - \hat{\theta}_r + \phi)}{2\left(\frac{{Z_{ha}}^2 - {Z_{hp}}^2 \sin^2 2(\theta_r - \hat{\theta}_r + \phi)}{4}\right)^2}.\end{aligned} \tag{7}$$

If the estimation error is small, $\hat{\theta}_r \approx \theta_r + \phi$, then the signal error can be approximated as follows:

$$\mathrm{Err} \approx \frac{{V_{dh}^*}^2 Z_{ha} Z_{hp}}{{Z_{ha}}^4}(\theta_r + \phi - \hat{\theta}_r) \equiv Y_{\mathrm{err}}(\theta_r + \phi - \hat{\theta}_r). \tag{8}$$

Also, if the deviation angle ϕ by stator current is compensated then the frequency response function relating the estimated and actual rotor angles is as follows:

$$\frac{\hat{\theta}_e(s)}{\theta_e(s)} = \frac{K_1 s + K_2}{s^2 + K_1 s + K_2} \tag{9}$$

where the correction controller $G(s) = \frac{1}{s}\left(K_P + \frac{K_I}{s}\right)$; $K_1 = Y_{\mathrm{err}} K_P$; and $K_2 = Y_{\mathrm{err}} K_I$.

The compensator is based on the characteristics of torque and high-frequency characteristics of an IPMM. If the high dynamics are required, the d-axis current command should be positive and the injection level high. The dynamics due to the increased gains may be fast but torque per current becomes low. If high torque per current is required, it is the opposite case. The compensation for the shifted angle are performed based on the offline test results.

IV. Initial Angle Detection Scheme

In the case of an induction motor, the flux position is decided by the controller because the flux-producing current, not by magnetic materials, generates the flux. However, in the case of an IPMM, the flux position is mechanically determined by the rotor position. For estimation of the magnetic pole position at the initial state, the conventional method has used the phenomenon of the saturation. The proposed method uses the harmonics of the high-frequency injection signal. In the case of an IPMM, the north magnetic pole position can be estimated by the hysteresis due to rotor flux saturation and its physical response

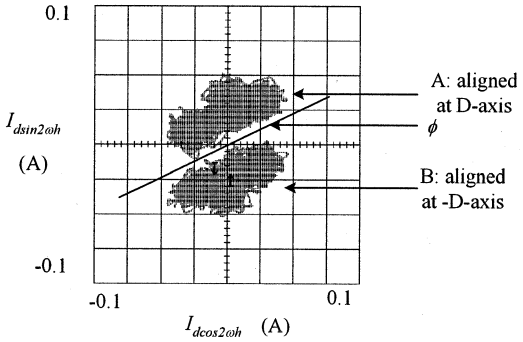

Fig. 5. Characteristics of second-order harmonic component of injected signal.

on the iron material. If the high-frequency signal is injected at the d-axis, the injected signal is distorted due to the hysteresis and then the distorted waveform has the even-order harmonics. Since the second-order harmonics are especially effective, these can be used in order to detect the d-axis. This method has the fast dynamics compared to the conventional method because the high-frequency signal is used. Fig. 5 shows the characteristics of the second-order harmonics of the injected signal. Region "A" in Fig. 5 represents the trajectory of the second-order harmonics when the high-frequency signal is injected at the d-axis and the real magnetic pole is at the arbitrary position. Region "B" in Fig. 5 represents when the high-frequency signal is injected at the negative d-axis, which is identical to the south magnetic pole position. At this time, the signals related to the second-order harmonics can be calculated as follows:

$$i_{dsh}^r = BPF\left(i_{ds}^r\right) \tag{10}$$

$$I_{d\sin 2\omega h} = 2LPF\left(i_{dsh}^r \cdot \sin 2\omega_h t\right) \tag{11}$$

$$I_{d\cos 2\omega h} = 2LPF\left(i_{dsh}^r \cdot \cos 2\omega_h t\right) \tag{12}$$

$$\phi = \tan^{-1}\frac{I_{d\sin 2\omega h}}{I_{d\cos 2\omega h}}. \tag{13}$$

When the phase of the second-order harmonics signal is between ϕ[rad] and $\phi + \pi$[rad], the flux angle is located at the positive d axis. Otherwise, the flux angle is located at the negative

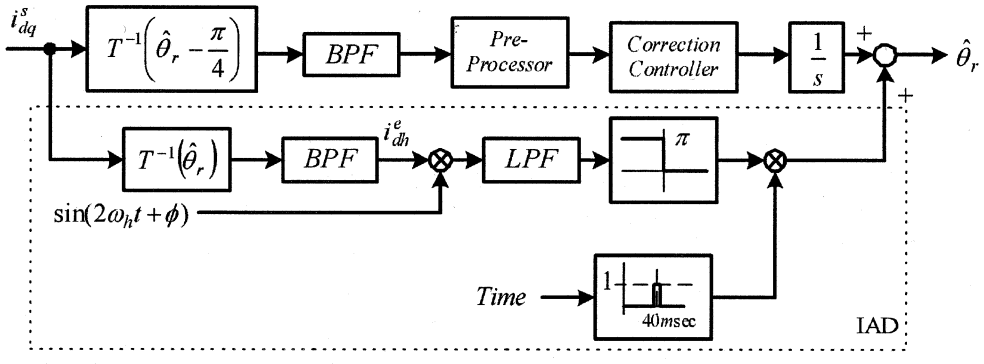

Fig. 6. Proposed method for initial angle detection.

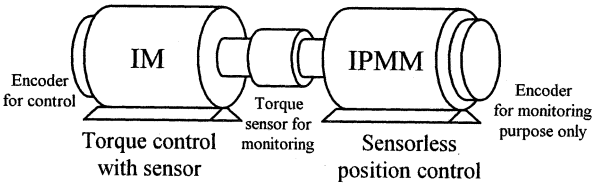

Fig. 7. System configuration for the experiments of the proposed sensorless control.

d axis. This can distinguish the north magnetic pole position in two magnetic pole positions.

The proposed method for initial angle detection is shown in Fig. 6. The proposed method largely consists of two parts. One is the estimation method for magnetic saliency using high-frequency signal injection and the other is the identification algorithm for the north magnetic pole position, which means the initial angle. The initial angle is estimated using the characteristics of the second-order harmonics of the injected signal and the high-frequency injection method proposed in [11], [12]. In the proposed method, the phase of the second-order harmonics in the injected signal is calculated as the following equation, which is the one-step signal process different from (10)–(13):

$$I_{d\sin 2\omega h\phi} = 2^* LPF\left(BPF\left(I^e_{ds}\right) \cdot \sin(2\omega_h t + \phi)\right). \quad (14)$$

This process can simply identify the d axis from d and $-d$ axes as follows. If the detected angle aligns at the positive d axis, $I_{d\sin 2\omega h\phi}$ is positive. If $I_{d\sin 2\omega h\phi}$ is negative, the estimated angle is compensated by adding π[rad]. After the d axis is identified once, the high-frequency injection method, which can operate in the low-speed region including zero speed, is ready to control the magnetic pole position..

V. Experimental Results

The system configuration for the experiments of the proposed sensorless position control is shown in Fig. 7. The digitally controlled pulsewidth-modulation (PWM) voltage-source inverter (VSI) system whose switching frequency is 5 kHz is used for this experiment and its main processor is a TMS320C31. For the experiment of the sensorless control of an IPMM whose parameters are listed in Table I, an induction motor is running in the torque control and the IPMM, which is under test, is in the position control mode with the proposed sensorless control algorithm. A torque transducer to monitor the load torque is installed between the two motors.

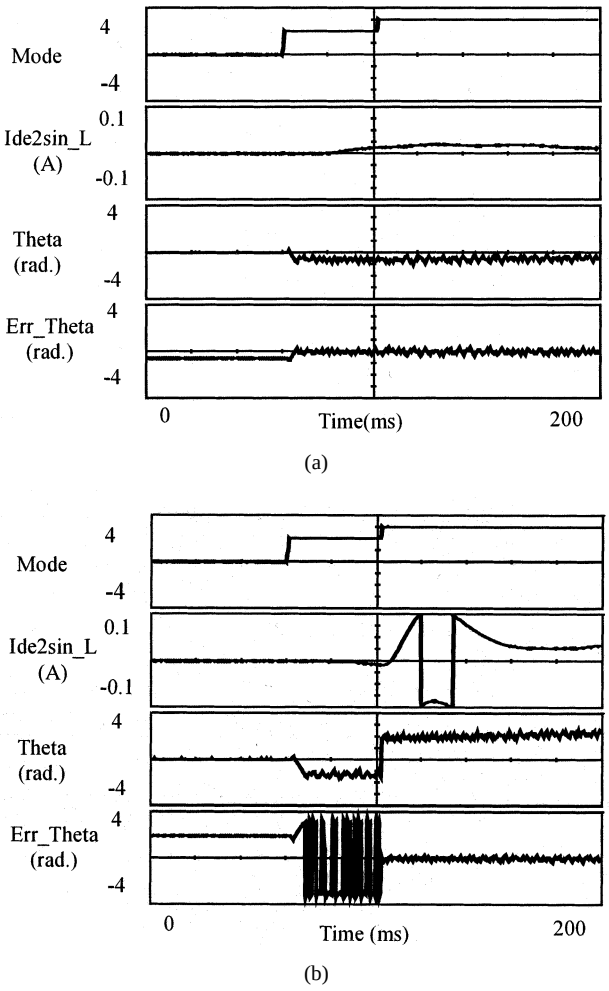

Fig. 8. Waveforms in initial angle detection. (a) When the estimated angle is at d axis. (b) When the estimated angle is at $-d$ axis.

Fig. 8 shows the experimental results of initial angle detection. In Fig. 8(a), the control angle need not be compensated because the estimated angle aligns at the positive d axis. In Fig. 8(b), the control angle must be compensated by π[rad] because the estimated angle aligns at the negative d axis. Modes 0, 2, and 3 represents turn-off state, initial angle detection

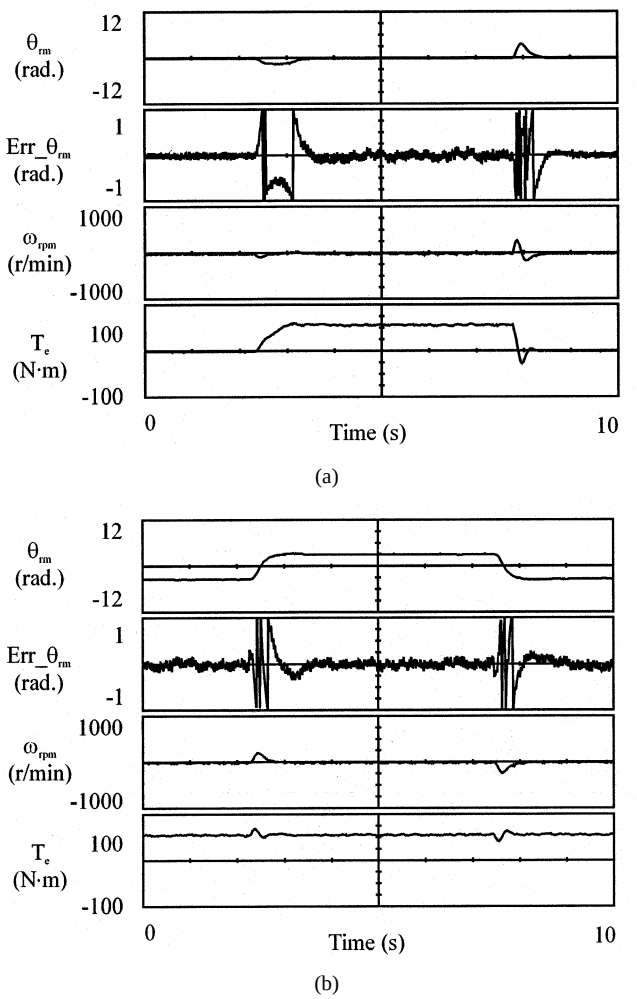

Fig. 9. Response of proposed sensorless position controller. (a) Zero position control under 100% step load variation. (b) Step change of position command from $-\pi$ rad to π rad and back to $-\pi$ rad under 100% load torque.

mode, and normal operation mode, respectively. In Fig. 8(b), at starting, the estimated angle is settled at the negative d axis. Before the compensation, the estimated angle is around π[rad], where it is the same with $-\pi$[rad] and it shows an overscaled condition in Fig. (8b). Then, after 40 ms, the error of the estimated angle is compensated by the proposed methods.

Fig. 9 shows the responses of the proposed sensorless position controller. The measured rotor position, the error of position, the measured rotor speed, and the measured torque are illustrated in each figure. Fig. 9(a) shows the response at zero position command when 100% step load is applied. Fig. 9(b) shows the step change of position command from $-\pi$ rad to π rad under 100% load condition. Even if the system is under the load, the steady-state position error of the proposed algorithm is bounded to a small value.

VI. Conclusion

IPMMs have originally magnetic saliency but it varies according to load conditions. In this paper, the saliency or impedance difference has been analyzed experimentally. This enables zero- or low-speed operation of a transducerless or position-sensorless IPMM. For the proposed algorithm, the characteristics of the IPMM are analyzed. A high-frequency injection scheme to amplify the difference containing the information of the rotor angle and to maintain the reasonable control performance under any load condition is proposed. It contains a scheme extracting the high-frequency impedance components related to the rotor position. In order to estimate the magnetic pole position, the high-frequency injection method is used. This method can estimate one of two magnetic pole positions. Then, the proposed method identifies the north magnetic pole position. The hysteresis phenomenon is utilized for the estimation. This has fast dynamics and can estimate the accurate magnetic pole position. The experimental results clarify the satisfactory operation of the sensorless position algorithm at zero and low speed from the initial state under any load condition.

References

[1] S. Ogasawara and H. Akagi, "An approach to position sensorless drive for brushless dc motor," *IEEE Trans. Ind. Applicat.*, vol. 27, pp. 928–933, Sept./Oct. 1991.

[2] K. D. Hurst, T. G. Habetler, G. Griva, and F. Profumo, "Zero-speed tacholess IM torque control: simply a matter of stator voltage integration," *IEEE Trans. Ind. Applicat.*, vol. 34, pp. 790–795, July/Aug. 1998.

[3] A. B. Kulkarni and M. Ehsani, "A novel position sensor elimination technique for interior permanent-magnet synchronous drive," *IEEE Trans. Ind. Applicat.*, vol. 28, pp. 144–150, Jan./Feb. 1992.

[4] R. B. Sepe and J. H. Lang, "Real-time observer-based (adaptive) control of a permanent-magnet synchronous motor without mechanical sensors," *IEEE Trans. Ind. Applicat.*, vol. 28, pp. 1345–1352, Nov./Dec. 1992.

[5] J. S. Kim and S. K. Sul, "High performance PMSM drives without rotational position sensors using reduced order observer," in *Conf. Rec. IEEE-IAS Annu. Meeting*, 1995, pp. 75–82.

[6] B.-J. Brunsbach, G. Henneberger, and T. Klepsch, "Position controlled permanent excited synchronous motor without mechanical sensors," in *Proc. EPE'93*, vol. 6, 1993, pp. 38–43.

[7] M. Schroedl, "Sensorless control of AC machines at low speed and standstill based on the 'INFORM' method," in *Conf. Rec. IEEE-IAS Annu. Meeting*, 1996, pp. 270–277.

[8] S. Ogasawara and H. Akagi, "Implementation and position control performance of a position-sensorless IPM motor drive system based on magnetic saliency," *IEEE Trans. Ind. Applicat.*, vol. 34, pp. 806–812, July/Aug. 1998.

[9] P. L. Jansen and R. D. Lorenz, "Transducerless position and velocity estimation in induction and salient AC machines," *IEEE Trans. Ind. Applicat.*, vol. 31, pp. 240–247, Mar./Apr. 1995.

[10] M. J. Corley and R. D. Lorenz, "Rotor position and velocity estimation for a permanent magnet synchronous machine at standstill and high speeds," in *Conf. Rec. IEEE-IAS Annu. Meeting*, vol. 1, 1996, pp. 36–41.

[11] J. I. Ha and S. K. Sul, "Sensorless field-orientation control of an induction machine by high-frequency signal injection," *IEEE Trans. Ind. Applicat.*, vol. 35, pp. 45–51, Jan./Feb. 1999.

[12] J. I. Ha, S. J. Kang, and S. K. Sul, "Position-controlled synchronous reluctance motor without any rotational transducer," *IEEE Trans. Ind. Applicat.*, vol. 35, pp. 1393–1398, Nov./Dec. 1999.

[13] J. M. Kim, S. J. Kang, and S. K. Sul, "Vector control of interior permanent magnet synchronous motor without a shaft sensor," in *Conf. Rec. IEEE APEC'97*, vol. 2, 1997, pp. 743–748.

[14] T. Takeshita and N. Matsui, "Sensorless control and initial position estimation of salient-pole brushless dc motor," in *Proc. AMC'96*, vol. 1, 1996, pp. 18–23.

[15] J. S. Kim and S. K. Sul, "New stand-still position detection strategy for PMSM drive without rotational transducers," in *Proc. IEEE APEC'94*, vol. 1, 1994, pp. 363–369.

[16] T. Noguchi, K. Yamada, S. Kondo, and I. Takahashi, "Initial rotor position estimation method of sensorless PM synchronous motor with no sensitivity to armature resistance," *IEEE Trans. Ind. Electron.*, vol. 45, pp. 118–125, Feb. 1998.

Jung-Ik Ha (S'97–M'01) was born in Pusan, Korea, in 1971. He received the B.S., M.S., and Ph.D. degrees in electrical engineering from Seoul National University, Seoul, Korea, in 1995, 1997, and 2001, respectively.

He was with the Mechatronics R&D Department, Yaskawa Electric Company, Japan, as a Researcher from 2001 to 2002. He is currently with the Mechatronics Center, Samsung Electronics Company, Gyeonggi, Korea, as a Senior Research Engineer. His current research interests are electric machines, their drives, and electric propulsion systems.

Kozo Ide (S'92–M'96) received the B.S., M.S., and Ph.D. degrees in electrical engineering from Kyushu Institute of Technology, Kitakyushu, Japan, in 1991, 1993, and 1996, respectively.

From 1991 to 1992, he was a Visiting Researcher at L'Aquila University, Italy, supported by the Italian government. In 1996, he joined Yaskawa Electric Company, Kitakyushu, Japan, where he is currently a Staff Engineer in the Mechatronics R&D Department. In 2002, he was a Visiting Researcher at Siemens AG, Germany. His current research interests are control technology for ac machines and energy conversion systems.

Dr. Ide is a Member of the Institute of Electrical Engineers of Japan.

Toshihiro Sawa (M'88) was born in Kochi Prefecture, Japan, in 1949. He received the M.S. degree in electrical and electronics engineering from Sophia University, Tokyo, Japan, in 1975.

In 1975, he joined Yaskawa Electric Company, Saitama, Japan, where he was engaged in the development and design of adjustable-speed ac motor drives. He is currently Manager of the Business Planning Department of the Motion Control Division and a Director.

Mr. Sawa is a Member of the Institute of Electrical Engineers of Japan.

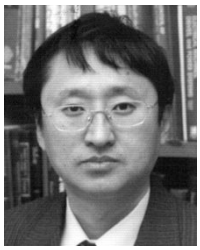

Seung-Ki Sul (S'78–M'87–SM'98–F'00) was born in Korea in 1958. He received the B.S., M.S., and Ph.D. degrees in electrical engineering from Seoul National University, Seoul, Korea, in 1980, 1983, and 1986, respectively.

He was with the Department of Electrical and Computer Engineering, University of Wisconsin, Madison, as an Associate Researcher from 1986 to 1988. He then was with Gold-Star Industrial Systems Company as a Principal Research Engineer from 1988 to 1990. Since 1991, he has been a member of the faculty of the School of Electrical Engineering and Computer Science, Seoul National University, where he is currently a Full Professor. His current research interests are electric machines, electric vehicles, and custom power and power converter circuits.